

# Manifold Oblique Random Forests: Closing the Gap to Convolutional Deep Networks

Ronan Perry<sup>1</sup>, Tyler M. Tomita<sup>1</sup>, Ronak Mehta<sup>1</sup>, Jesus Arroyo<sup>2</sup>, Jesse Patsolic<sup>1</sup>, Benjamin Falk<sup>1</sup>,  
Joshua T. Vogelstein<sup>1,2,3\*</sup>

**Abstract.** Decision forests (DFs), in particular random forests and gradient boosting trees, have demonstrated state-of-the-art accuracy compared to other methods in many supervised learning scenarios. In particular, DFs dominate other methods in tabular data, that is, when the feature space is unstructured, so that the signal is invariant to permuting feature indices. However, in structured data lying on a manifold—such as images, text, and speech—deep networks (DNs), specifically convolutional deep networks (ConvNets), tend to outperform DFs. We conjecture that at least part of the reason for this is that the input to DNs is not simply the feature magnitudes, but also their indices (for example, the convolution operation uses “feature locality”). In contrast, naïve DF implementations fail to explicitly consider feature indices. A recently proposed DF approach demonstrates that DFs, for each node, implicitly sample a random matrix from some specific distribution. These DFs, like some classes of DNs, learn by partitioning the feature space into convex polytopes corresponding to linear functions. We build on that approach and show that one can choose distributions in a *manifold-aware fashion* to incorporate feature locality. We demonstrate the empirical performance on data whose features live on three different manifolds: a torus, images, and time-series. In all simulations, our Manifold Oblique Random Forest (M<sub>ORF</sub>) algorithm empirically dominates other state-of-the-art approaches that ignore feature space structure and challenges the performance of ConvNets. Moreover, M<sub>ORF</sub> runs significantly faster than ConvNets and maintains interpretability and theoretical justification. This approach, therefore, has promise to enable DFs and other machine learning methods to close the gap to deep networks on manifold-valued data. Our code is open source and available at <https://github.com/neurodata/SPORF/>.

**1 Introduction** Decision forests, including random forests and gradient boosting trees, have solidified themselves in the past couple decades as a powerful ensemble learning method in supervised settings [1, 2], including both classification and regression [3]. In classification, each forest is a collection of decision trees whose individual classifications of a data point are aggregated together using majority vote. One of the strengths of this approach is that each decision tree need only perform better than chance for the forest to be a strong learner, given a few assumptions [4, 5]. Additionally, decision trees are relatively interpretable because they can provide an understanding of which features are most important for correct classification [6]. Breiman originally proposed decision trees that partition the data set using hyperplanes aligned to feature axes [6]. Yet, this limits the flexibility of the forest and requires trees of large depth to classify some data sets, leading to overfitting. He also suggested that algorithms which partition based on sparse linear combinations of the coordinate axes can improve performance [6]. More recently, Sparse Projection Oblique Randomer Forest (SPORF) partitions a random projection of the data and has shown impressive improvement over other methods [7].

Yet random forests and other machine learning algorithms frequently operate in a tabular setting, viewing an observation  $\vec{x} = (x_1, \dots, x_p)^\top \in \mathbb{R}^p$  as an unstructured feature vector. In doing so, they neglect the indices in settings where the indices encode additional information. For structured data, e.g. images or time series, traditional decision forests are not able to incorporate known continuity between features to learn new features. For decision forests to utilize known local structure in data, new features encoding this information must be manually constructed or new splitting criterion must be implemented. Prior research has extended random forests to a variety of computer vision tasks [8–11] and augmented random forests with structured pixel label information [12]. The decision tree at the heart of the Microsoft Kinect showed great success by specializing for image data with depth information [11]. Yet these methods either generate features *a priori* from individual pixels, and thus do not take advantage of the local topology, or lack the flexibility to learn relevant structure. Decision forests have been used to learn distance metrics on unknown manifolds [13], but such manifold forest algorithms are unsupervised and aim to learn a low dimensional representation of the data.

Inspired by SPORF, we propose a projection distribution that takes into account neighboring fea-

\* <sup>1</sup> Department of Biomedical Engineering Johns Hopkins University, <sup>2</sup> Center for Imaging Science, <sup>3</sup> Institute for Computational Medicine, Kavli Neuroscience Discovery Institute, Johns Hopkins University

tures while incorporating enough randomness to learn the relevant projections. At each node in the decision tree, a set of neighboring features are randomly selected using knowledge of the underlying manifold. Weighting and summing the values of the selected features yields a set of oblique projections of the data which can then be evaluated to partition the observations. We describe this proposed classification algorithm, Manifold Oblique Random Forests (MF) in detail and show its effectiveness in three simulation settings as compared to common classification algorithms. Furthermore, the optimized and parallelizable open source implementation of MF in Python is available. This addition makes for an effective and flexible learner across a wide range of manifold structures.

## 2 Background and Related Work

**2.1 Classification** Let  $(X, Y) \in \mathcal{X} \times \mathcal{Y}$  be a random sample from the joint distribution  $F_{XY}$  and  $D_n := \{(x_i, y_i)\}_{i=1}^n$  be our observed data where  $(x_i, y_i) \in \mathcal{X} \times \mathcal{Y}$  is drawn from  $F_{XY}$  for all  $i$ .  $\mathcal{X} \subseteq \mathbb{R}^p$  (the space of feature vectors), and  $\mathcal{Y} = \{1, \dots, K\}$  (the space of class labels). A classifier is a function that assigns to  $X$  a class label  $y \in \mathcal{Y}$ . Our goal is to learn a classifier  $g_n(X; D_n) : \mathcal{X} \times (\mathcal{X} \times \mathcal{Y})^n \rightarrow \mathcal{Y}$  from our data that minimizes the expected risk corresponding to 0 – 1 loss, the probability of incorrect classification,

$$L(g) := \mathbb{E}[\mathbb{I}[g(X) \neq Y]] = P(g(X) \neq Y),$$

with respect to the distribution of  $(X, Y)$ . The optimal such classifier is the Bayes classifier

$$g^*(X) := \operatorname{argmax}_{y \in \{1, \dots, K\}} P(Y = y | X),$$

which has the lowest attainable risk  $L^* := L(g^*(X))$ . For some finite number of samples  $n$ , our goal is to learn a classifier  $g_n$  from the data  $D_n$  that performs well with error denoted by  $L_n := L(g_n(X)) = P(g_n(X) \neq Y)$ .

**2.2 Random Forests** Originally popularized by Breiman, the random forest (RF) classifier is empirically very effective [1] while maintaining strong theoretical guarantees [6]. A random forest is an ensemble of decision trees whose individual classifications of a data point are aggregated together using majority vote. Each decision tree consists of split nodes and leaf nodes. A split node is associated with a subset of the data  $S = \{(x_i, y_i)\} \subseteq D_n$  and splits into two child nodes, each associated with a binary partition of  $S$  based on the value of the  $j$ th feature. Let  $e_j \in \mathbb{R}^p$  denote a unit vector in the standard basis (that is, a vector with a single one in the  $j$ th entry and the rest of the entries are zero) and  $\tau$  a threshold value. Then  $S$  is partitioned into the two subsets

$$\begin{aligned} S_\theta^L &= \{(x_i, y_i) | e_j^\top x_i < \tau\}, \\ S_\theta^R &= \{(x_i, y_i) | e_j^\top x_i \geq \tau\}. \end{aligned}$$

given the pair  $\theta = \{e_j, \tau\}$ . To choose the partition, the optimal  $\theta^* = (e_j^*, \tau^*)$  pair is selected via a greedy search from among a set of  $d$  randomly selected standard basis vectors  $e_j$ . The selected partition is that which maximizes some measure of information gain. A typical measure is a decrease in impurity, calculated by the Gini impurity score  $I(S)$ , of the resulting partitions [3]. Let  $\hat{p}_k = \frac{1}{|S|} \sum_{y_i \in S} \mathbb{I}[y_i = k]$  be the fraction of elements of class  $k$  in partition  $S$ , then the optimal split is found as

$$\theta^* = \operatorname{argmax}_\theta |S|I(S) - |S_\theta^L|I(S_\theta^L) - |S_\theta^R|I(S_\theta^R),$$

where  $I(S) = \sum_{k=1}^K \hat{p}_k(1 - \hat{p}_k)$ . A leaf node in the decision tree is created once a partition reaches a stopping criterion, typically either falling below an impurity score threshold or a minimum number of observations [3].

To classify a sample  $x$ , it is evaluated at root node of the tree and split into one of the two partitions. This process is repeated recursively at subsequent split nodes until  $x$  "falls into" a leaf, upon which

posterior probability estimates of the class labels can be assigned. Let  $l_b(x)$  be the set of training examples at the leaf node in tree  $b$  into which  $x$  falls. The empirical posterior probability of label  $y$  in  $b$  is thus  $p_{nb}(y | x) = \frac{1}{|l_b(x)|} \sum_{i=1}^n \mathbb{I}[y_i = y] \mathbb{I}[x_i \in l_b(x)]$ . The forest composed of  $B$  trees computes the empirical posterior probability for  $x$  by averaging over the trees  $p_n(y | x) = \frac{1}{B} \sum_{b=1}^B p_{nb}(y | x)$  and classifies  $x$  per the label with the greatest empirical posterior probability [3]

$$g_n(x) = \operatorname{argmax}_{y \in \{1, \dots, K\}} p_n(y | x)$$

For good performance of the ensemble and strong theoretical guarantees, the individual decision trees must be relatively uncorrelated from one another. Breiman's random forest algorithm does this in two ways:

1. At every node in the decision tree, the optimal split is determined over a random subset  $d$  of the total collection of features  $p$ .
2. Each tree is trained on a randomly bootstrapped sample of data points  $D' \subset D_n$  from the full training data set.

Applying these techniques reduces the capability of random forests to overfit and lowers the upper bound of the generalization error [6].

**2.3 Sparse Projection Oblique Randomer Forests**  $\text{SPORF}$  is a recent modification to random forest that has shown improvement over other versions [7, 14]. Recall that RF split nodes partition data along the coordinate axes by comparing the projection  $e_j^\top x$  of observation  $x$  on standard basis  $e_j$  to a threshold value  $\tau$ .  $\text{SPORF}$  generalizes the set of possible projections, allowing for the data to be partitioned along axes specified by any sparse vector  $a_j$ . The partition

$$\begin{aligned} S_\theta^L &= \{(x_i, y_i) \mid a_j^\top x_i < \tau\}, \\ S_\theta^R &= \{(x_i, y_i) \mid a_j^\top x_i \geq \tau\} \end{aligned}$$

follows from our choice of  $\theta = \{a_j, \tau\}$ . Rather than partitioning the data solely along the coordinate axes (i.e. the standard basis),  $\text{SPORF}$  creates partitions along axes specified by sparse vectors. In other words, let the dictionary  $\mathcal{A}$  be the set of atoms  $\{a_j\}$ , each atom a  $p$ -dimensional vector defining a possible projection  $a_j^\top x$ . In axis-aligned forests,  $\mathcal{A}$  is the set of standard basis vectors  $\{e_j\}$ . In  $\text{SPORF}$ , the dictionary  $\mathcal{A}$  can be much larger, because it includes, for example, all 2-sparse vectors. At each split node,  $\text{SPORF}$  samples  $d$  atoms from  $\mathcal{A}$  according to a specified distribution. By default, each of the  $d$  atoms are randomly generated with a sparsity level drawn from a Poisson distribution with a specified rate  $\lambda$ . Then, each of the non-zero elements are uniformly randomly assigned either  $+1$  or  $-1$ . Note that the size of the dictionary for  $\text{SPORF}$  is  $3^p$  (because each of the  $p$  elements could be  $-1$ ,  $0$ , or  $+1$ ), although the atoms are sampled from a distribution heavily skewed towards sparsity.

### 3 Methods

**3.1 Random Projection Forests on Manifolds** In the structured setting, the dictionary of projection vectors  $\mathcal{A} = \{a_j\}$  is modified to take advantage of *a priori* knowledge of the underlying manifold on which the data lie. We term this method the Manifold Oblique Random Forest (MF). This modification constrains the space of random projection decision trees which can be learned in order to better suit certain classification tasks. The individual trees are ensembled using majority vote from the component decision tree predictions, as in RF.

Let  $\mathcal{A}$  be a dictionary of  $m$ ,  $p$ -dimensional weight vectors (atoms) with probability density or mass function  $f_{\mathcal{A}}$  over the  $m$  atoms. Each atom  $a_j \in \mathcal{A}$  projects an observation  $x_i$  to a real number  $a_j^\top x_i$ , where nonzero elements of  $a_j$  effectively weight and sum features. A sampled set of  $d$  atoms form the rows of projection matrix  $A \in \mathbb{R}^{p \times d}$  and  $A^\top x_i \in \mathbb{R}^d$  is the collection of  $d$  projected features. At each node in the decision tree, MF samples such a matrix  $A$  and selects the best split according to the Gini index over each projected feature across all samples to grow the tree on. Unlike other oblique

random forests, however, MF is tailored to a setting where the features of an observation  $x_i \in \mathbb{R}^p$  lie on a manifold, inducing a notion of feature locality. Such relations between features may be indicative information in certain classification tasks. For instance, edges in images or spikes in time-series may be identified by values in a neighborhood of pixels or times, respectively. The atoms in  $\mathcal{A}$  are restricted to those which make sense given the feature locality, whereas other oblique random forests are allowed to sample unrestricted.

In our implementation, we view the features of an observation  $x_i \in \mathbb{R}^p$  as an unraveled 2D matrix in  $\mathbb{R}^{W \times H}$ . A "patch" is a rectangular subset of this 2D matrix reminiscent of a convolutional filter, defined by its height, width, and upper-left corner index. All features within the patch are summed to produce a candidate univariate feature to split on. Thus, a patch corresponds to a unique atom  $a \in \mathbb{R}^p$  where  $a_i = 1$  if  $i$  is in the patch and  $a_i = 0$  otherwise; the candidate feature is calculated through sparse matrix multiplication.

At each split node, a set of rectangular patches are randomly sampled to produce candidate features across observations. MF accepts hyperparameters defining the minimum and maximum patch heights  $\{h_{min}, h_{max}\}$  and widths  $\{w_{min}, w_{max}\}$ , respectively. To sample a patch, first the height ( $h$ ) and width ( $w$ ) are independently and uniformly sampled,

$$\begin{aligned} h &\sim \text{unif}\{h_{min}, h_{max}\} \\ w &\sim \text{unif}\{w_{min}, w_{max}\}, \end{aligned}$$

between respective minima and maxima inclusively. Then the upper-left corner location  $(u, v)$  is uniformly sampled,

$$\begin{aligned} u &\sim \text{unif}\{-h + 1, H\} \\ v &\sim \text{unif}\{-w + 1, W\}, \end{aligned}$$

among all features and a zero-padded boundary which can be entirely ignored by  $a$  as it contributes nothing to the weighted sum. The zero-padded region exists so that each feature has an equally likely chance of being contained in the rectangle given the sampled dimensions. Algorithm pseudocode can be found in Appendix B which is equivalent to SPORF except for the distribution  $f_{\mathcal{A}}$  described above [7].

The structure of these atoms is flexible and task dependent. Our atoms were limited to values of 1 and 0 to limit combinatorial complexity but domain-specific atom design may be desired in some settings. For graph-valued data, one may consider sampling a collection of neighboring edges or nodes [15]. In the case of data lying on a cyclic manifold, as in the first experiment we conduct, the atoms are patches that "wrap-around" borders of the matrix to capture added continuity. In the case of multi-channel time-series data, neighboring points in the time domain are selected but sampling of multiple channels faces no structural restrictions. We pose a single channel experiment later as well. By constructing features in this way, MF learns low-level features in the structured data, such as corners in images or spikes in time-series. The forest can therefore learn the features that best distinguish a class.

An important aspect of this method is that MF represents a shift to more "locally connected" tools whereby local points provide relevant information. However, unlike ConvNets, this method is not translation invariant. Thus, discriminative features must be constant in their indices or the training data must be rich enough to fully encapsulate possible observations [11].

**3.2 Feature Importance** One of the benefits to decision trees is that their results are fairly interpretable in that they allow for estimation of the relative importance of each feature. Many approaches have been suggested [6, 16] and here a projection forest specific metric is used in which the number of times a given feature was used in projections across the ensemble of decision trees is counted. A decision tree  $T$  is composed of many nodes  $j$ , each one associated with an atom  $a_j^*$  and threshold that partition the feature space according to the projection  $a_j^{*T}x$ . Thus, the indices corresponding to non-zero elements of  $a_j^*$  indicate important features used in the projection. For each feature  $k$ , the number

of times  $\pi_k$  it is used in a projection, across all split nodes and decision trees, is counted.

$$\pi_k = \sum_T \sum_{j \in T} \mathbb{I}(a_{jk}^* \neq 0)$$

These normalized counts represent the relative importance of each feature in making a correct classification. Such a method applies to both  $\text{SPORF}$  and  $\text{MF}$ , although different results between them would be expected due to different distributions and dictionaries.

## 4 Theoretical Results

**4.1 Partitioning of the Feature Space** We note, that  $\text{SPORF}$  and all other oblique forests have certain nice properties, such as the following result. Further details can be found in the Appendix.

**Theorem 1.** *A decision tree formed from oblique splits partitions the feature space into a finite number of (possibly unbounded) convex polytopes.*

Each polytope region corresponds to a leaf node and a constant classification label per the samples used to populate that leaf. This result is of interest as it has been shown that deep nets with Rectified Linear Units (ReLUs) or hard tanh activation layers also partition the feature space into convex polytopes with different linear functions on each region [17]. Indeed, this shared "partition and vote scheme" offers insight into their relationship with one another as well as the functioning of the brain [18]

**4.2 Classifier Consistency** The least we can ask of a classification rule is for it to be consistent. That is, the probability of misclassification converges to the minimum (Bayes) error of misclassification. Random projection forests are well-behaved in that they maintain and hold certain desired statistical properties from the literature of axis-aligned splits. *Honesty* is a mild constraint that requires the set of training examples used to learn the structure of the tree to be independent of the set of examples used at the leaf nodes to estimate the posterior probabilities and has been used to prove asymptotic results about forests [5, 19–21].

Following from the results of Athey et al. [21], we adopt this constraint and show that appropriately constructed honest random projection forests produce consistent classification rules given a few general assumptions, see Appendix for details. We denote as before  $x \in \mathcal{X} \subseteq \mathbb{R}^p$  and  $y \in [1, \dots, K]$ . From the following assumptions, we have one of our main results.

### Assumptions

1. The dictionary  $\mathcal{A}$  is finite and contains the set of standard basis vectors  $\{e_i\}_{i=1}^p$ , each with a fixed nonzero probability of being selected at each split node.
2. For all  $y \in \mathcal{Y}$ ,  $P(Y = y \mid X = x)$  is Lipschitz continuous in  $x \in \mathcal{X}$ .
3. The samples used to populate the leaves of the trees are mutually exclusive from the set used to learn the structure of the trees (Honesty).
4. There exists a density  $f$  over  $\mathcal{X}$  and for all  $x \in \mathcal{X}$  there exists a  $\varepsilon > 0$  such that  $\varepsilon < f(x) < \frac{1}{\varepsilon}$ .

**Theorem 2.** *Under Assumptions 1-4, the classification rule from an honest random forest making oblique splits from the dictionary  $\mathcal{A}$  and built to the specifications of  $\text{SPORF}$  is consistent, i.e.*

$$L_n \xrightarrow{P} L^* \quad \text{as } n \rightarrow \infty$$

The Lipschitz assumption is a valid one taken in the literature on random forests [21]. It intuitively makes sense *a priori* that small deviations in  $x$  should lead to small deviations in the class probability. Theorem 2 tells us that honest  $\text{SPORF}$  is consistent, but from the flexibility of the dictionary  $\mathcal{A}$  the following corollary is clear.

**Corollary 1.** *Under the conditions of Theorem 2, honest  $\text{MF}$  yields a consistent classification rule.*

Like axis-aligned splits, oblique splits partition the feature space into convex polytopes whose radii go to zero, but slow enough to populate the leaves with sets of size going to infinity.



**4.3 Time and Space Complexity** Theoretical analysis of decision tree complexity is difficult without making assumptions on the data as a tree’s possible structure occupies a combinatorially large space. While the worst case may not be expected, the bound it presents is too large to be helpful in typical scenarios. We examine a simplified average setting in which the possible sizes induced at each partition node are equally likely. It has been posited and supported empirically that this is a lower bound for the true average case in a RF [22]. One reason that worse-than average cases may occur is that when none of the candidate features are informative, edge splits are frequent and lead to deep trees [22]. The candidate features in  $\text{SPORF}$  and  $\text{MF}$  are combinations of individual features and we expect this greater flexibility to reduce the chance that no features are informative.

Let a forest have  $T$  trees,  $d$  candidate features at each split node (i.e.  $m_{\text{try}}$ ), and  $n$  training samples. At each split node in RF, the complexity is  $O(dn \log n)$  to sort observations along each feature using an optimal sorting algorithm [22]. In the average case, the training time complexity for RF is then  $O(Tdn \log^2 n)$  [22].  $\text{MF}$ , as well as  $\text{SPORF}$ , utilize sparse matrix multiplication to compute the weighted sums while sorting observations at split nodes. Thus, letting  $H$  and  $W$  denote the maximum height and width of a patch in  $\text{MF}$ , the training time complexity for  $\text{MF}$  is  $O(Td(HW)n \log^2 n)$ . However, as we will show empirically,  $\text{MF}$  can find better partitions and thus learn smaller trees. Note that random forests are embarrassingly parallelizable and the scaling in  $T$  can be scaled down linearly by the number of processors in parallel.

In terms of storage space complexity, for a classification problem with  $c$  classes the theoretical complexity of  $\text{SPORF}$  is  $O(T(np + c))$  since  $p$  dominates the number of nonzero atoms [7]. So it follows that  $\text{MF}$  also has a storage complexity of  $O(T(np + c))$  as it is invariant to the projections themselves.

**5 Simulation Experiments** We evaluate  $\text{MF}$  in three simulation settings to show its ability to take advantage of the structure in the data. It was compared to a set of traditional classifiers and  $\text{SPORF}$  that all learn from the raw features. For each experiment, we used our open source implementation of  $\text{MF}$  as well as  $\text{SPORF}$  and the RF implementation contained in the  $\text{SPORF}$ , each with 500 trees. Other classifiers were run from the Scikit-learn Python package [23] and the powerful gradient boosted tree XGBoost (XGB) was run using its Python implementation [24]. Additionally, we tested against a Convolutional Deep Network (ConvNet) built using PyTorch [25] with two convolution layers, ReLU activations, and maxpooling, followed by dropout and a densely connected hidden layer.

Method hyper-parameters were left as defaults except for the ConvNets and  $\text{MF}$  which are each specific to the structure of the data and so must be changed. Thus, a well-performing ConvNet architecture was selected and  $\text{MF}$  hyper-parameters were optimized using a grid search over a range of potential values for the minimum and maximum patch size as well as  $\text{max\_features}$  ( $m_{\text{try}}$ ) which is related to the combinatorial space of possible features determined by the patch size. See Appendix C for details on the hyperparameters and network architectures across experiments.

**5.1 Simulation Settings** Experiment (A) is a non-Euclidean cyclic manifold example inspired by Younes [26]. Each observation is a discretization of a circle into 100 features with two non-adjacent segments of  $1\hat{\text{A}}\hat{\text{Z}}$ s in two differing patterns: class 1 features two segments of length five while class 2 features one segment of length four and one of length six. Figure 1(A) shows examples from the two classes and classification results across various sample sizes.

Experiment (B) is a simple  $28 \times 28$  binary image classification problem. Images in class 0 contain randomly sized and spaced *horizontal* bars while those in class 1 contain randomly sized and spaced *vertical* bars. For each sampled image,  $k \sim \text{Poisson}(\lambda = 10)$  bars were distributed among the rows or columns, depending on the class. The distributions of the two classes are identical if a 90 degree rotation is applied to one of the classes. Figure 1(B) shows examples from the two classes and classification results across various sample sizes.

Experiment (C) is a signal classification problem. One class consists of 100 values of Gaussian

noise while the second class has an added exponentially decaying unit step beginning at time 20.

$$\begin{aligned} X_t^{(0)} &= \epsilon \\ X_t^{(1)} &= u(t - 20)e^{(t-20)} + \epsilon \\ \epsilon &\sim \mathcal{N}(0, 1) \end{aligned}$$

Figure 1(C) shows examples from the two classes and classification results across various sample sizes.

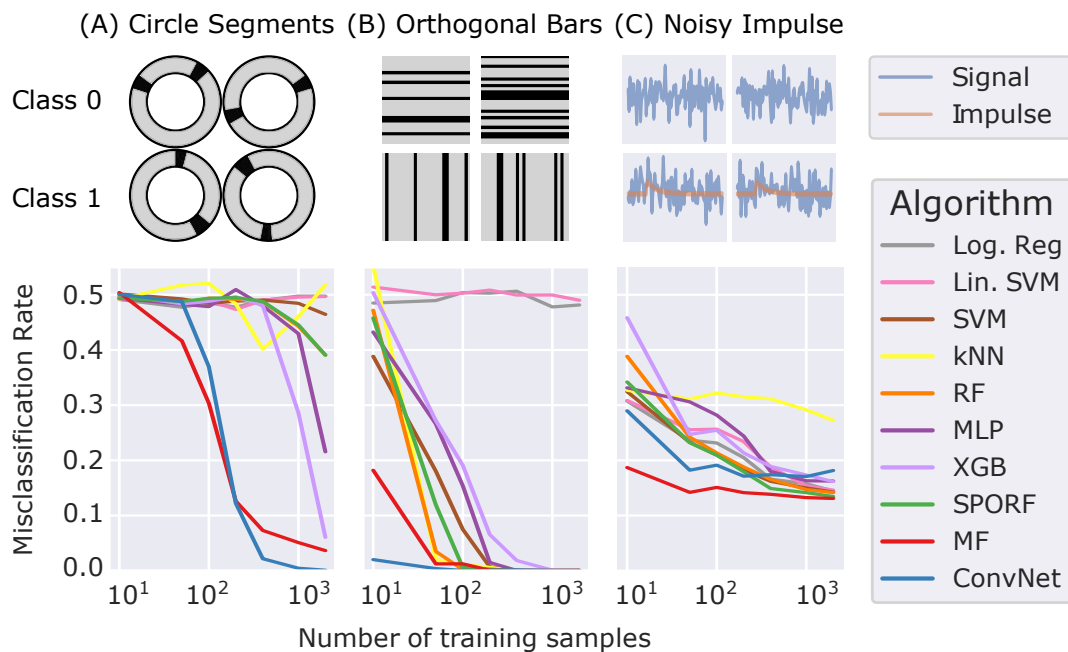


Figure 1: MF outperforms other algorithms in three two-class classification settings. Upper row shows examples of simulated data from each setting and class. Lower row shows misclassification rate in each setting, tested on 10,000 test samples. **(A)** Two segments in a discretized circle. Segment lengths vary by class. **(B)** Image setting with uniformly distributed horizontal or vertical bars. **(C)** White noise (class 0) vs. exponentially decaying unit impulse plus white noise (class 1).

**5.2 Results** In all three simulation settings, MF outperforms all other classifiers, doing especially better at low sample sizes, except the ConvNet for which there is no clear winner. The performance of MF is particularly good in the discretized circle simulation for which most other classifiers perform at chance levels. MF also performs quite well in the signal classification problem, most likely because of the ability to learn wide patch sizes which mimics the optimal classifier. Experiments with uniformly distributed atom weights in between 0 and 1 showed no improvement and so were omitted.

We compare the empirical complexity of MF, SPORF, and RF (from the SPORF package<sup>1</sup>) in Figure 2. Although projection forests required more computations at each partition node during training, as outlined in Section 4.3, MF is able to learn less complex trees in all cases and sample sizes.

Each simulated experiment was run on CPUs and allocated 45 cores for parallel processing. The resulting train and test times as a function of the number of training samples are plotted in Figure 3. MF has train and test times on par with those of SPORF and so is not particularly more computationally intensive to run. The ConvNet, however, took noticeably longer to run across simulations for the majority of sample sizes. Thus its strong performance in those settings comes at an added computational cost, a typical issue for deep learning methods [27].

<sup>1</sup><https://github.com/neurodata/SPORF/>

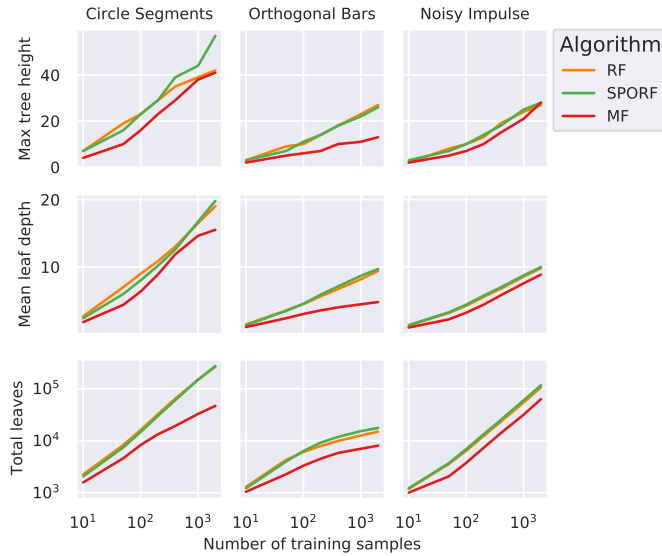


Figure 2: Random forest comparisons in each simulation on their maximum tree height, mean leaf depth, and total number of leaves. MF is able to learn simpler trees in all cases due to its tailored projection distribution.

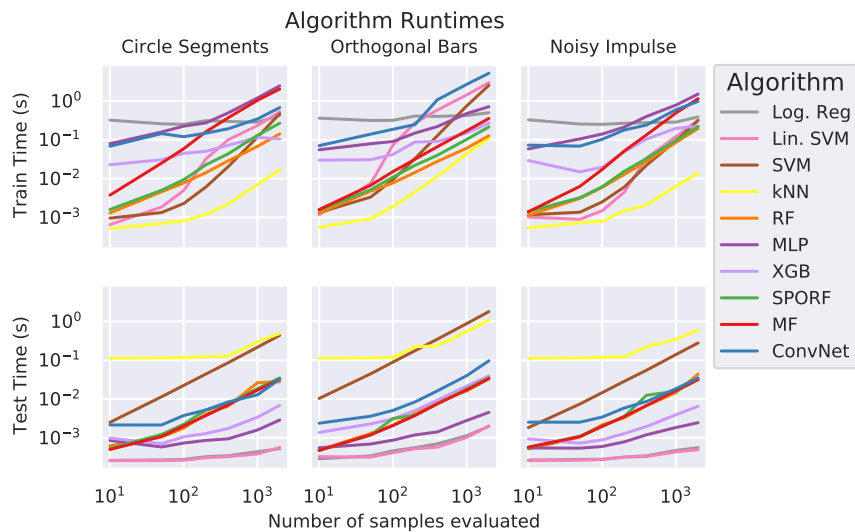


Figure 3: Algorithm train times (above) and test times (below) across increasing sample sizes. MF runtime is not particularly costly and well below ConvNet runtime in most examples.

## 6 MNIST Experiment

**6.1 Results** MF’s performance was evaluated on the MNIST dataset, a collection of handwritten digits stored in 28 by 28 square images [28], and compared to the algorithms used in the simulations. 10,000 images were held out for testing and the remaining images were used for training. The results are displayed in Figure 4. Hyperparameters are as described in the simulations, see Appendix C for details. MF showed an improvement over the other algorithms, especially for smaller sample sizes. Thus, even this trivial modification can improve performance by several percentage points. Specifically, MF achieved a lower classification error than all other algorithms besides the ConvNet for all sample sizes.



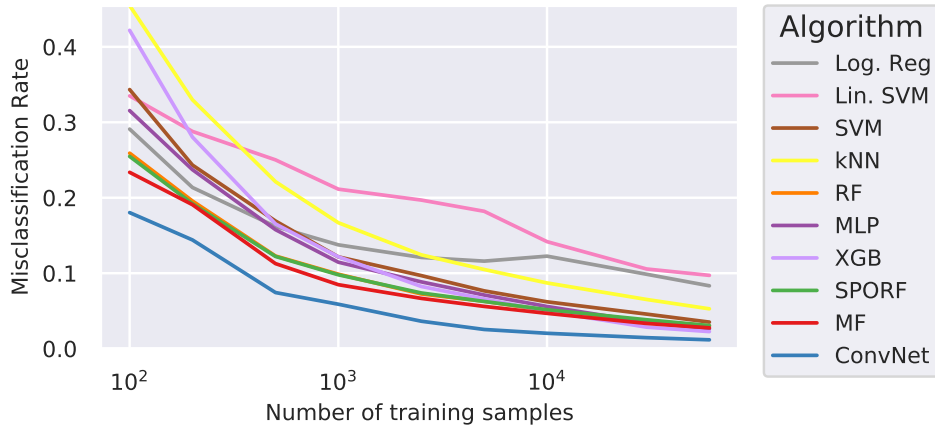


Figure 4: MF improves classification accuracy over all other non-ConvNet algorithms for all sample sizes, especially in small sample sizes.

**6.2 Feature Importance** To evaluate the capability of MF to identify importance features in manifold-valued data as compared to SFORF and RF. All methods were run on a subset of the MNIST dataset: we only used threes and fives, 100 images from each class.

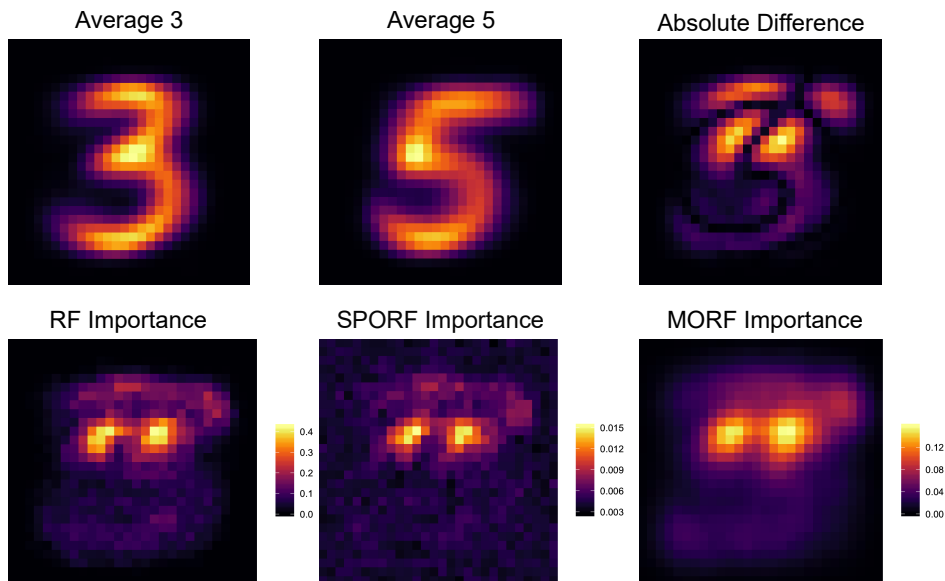


Figure 5: Averages of images in the two classes and their difference (above). Feature importance from MF (bottom right) shows less noise than SFORF (bottom middle) and is smoother than RF (bottom left).

The feature importance of each pixel is shown in Figure 5. MF visibly results in a smoother pixel importance, a result most likely from the continuity of neighboring pixels in selected projections. Although Tomita et al. [7] demonstrated empirical improvement of SFORF over RF on the MNIST data, its projection distribution yields scattered importance of unimportant background pixels as compared to RF. Since projections in SFORF have no continuity constraint, those that select high importance pixels will also select pixels of low importance by chance. This may be a nonissue asymptotically, but is a relevant problem in low sample size settings. MF, however, shows little or no importance of these background

pixels by virtue of the modified projection distribution.

**7 Discussion** The success of sparse oblique projections in decision forests has opened up many possible ways to improve axis-aligned decision forests (including random forests and gradient boosting trees) by way of specialized projection distributions. Traditional decision forests have already been applied to some manifold-valued data, using predefined features to classify images or pixels, and have shown great success but ignore pixel continuity and specialize for a specific data modalities. We expand upon sparse oblique projections and introduced manifold-aware projection distributions that uses prior knowledge of the topology of a feature space. The open source implementation of `SPORF` has allowed for the implementation of `MF`, creating a flexible classification method for a variety of data modalities and tailored projection dictionaries. We showed in various simulated settings that appropriate domain knowledge can improve the projection distribution to yield impressive results that challenge the strength of deep learning techniques on manifold-valued data. On the MNIST data set, `MF` closed the gap to ConvNets while maintaining interpretability, robustness to hyperparameter tuning, quick run time, and theoretical justification.

Research into other, task-specific projection dictionaries may lead to improved results in real-world computer vision tasks or classification tasks in other manifold-valued settings such as graphs. These projection distributions, while incorporated into `SPORF` here, may also be incorporated into other state of the art algorithms such as `XGBBOOST`. Additionally, the partition and vote framework of oblique forests opens interesting connections to deep networks and learning in general.

**8 Acknowledgements** This work is supported by the Defense Advanced Research Projects Agency (DARPA) Lifelong Learning Machines program through contract FA8650-18-2-7834 and through funding from Microsoft Research. The authors have no conflicts of interest to declare.

## References

- [1] Manuel Fernández-Delgado, Eva Cernadas, Senén Barro, and Dinani Amorim. Do we need hundreds of classifiers to solve real world classification problems? *Journal of Machine Learning Research*, 15:3133–3181, 2014.
- [2] Rich Caruana and Alexandru Niculescu-Mizil. An empirical comparison of supervised learning algorithms. In *Proceedings of the 23rd International Conference on Machine Learning, ICML '06*, pages 161–168, New York, NY, USA, 2006. ACM. ISBN 1-59593-383-2. doi: 10.1145/1143844.1143865.
- [3] Trevor Hastie, Robert Tibshirani, and Jerome Friedman. *The Elements of Statistical Learning*. Springer Series in Statistics. Springer New York Inc., New York, NY, USA, 2001.
- [4] Robert E. Schapire. The strength of weak learnability. *Mach. Learn.*, 5(2):197–227, July 1990. ISSN 0885-6125. doi: 10.1023/A:1022648800760.
- [5] Gerard Biau, Luc Devroye, and Gabor Lugosi. Consistency of Random Forests and Other Averaging Classifiers. *J. Mach. Learn. Res.*, 9:2015–2033, June 2008. ISSN 1532-4435.
- [6] Leo Breiman. Random forests. *Machine Learning*, 45(1):5–32, Oct 2001. ISSN 1573-0565. doi: 10.1023/A:1010933404324.
- [7] Tyler M. Tomita, James Browne, Cencheng Shen, Jesse L. Patsolic, Jason Yim, Carey E. Priebe, Randal Burns, Mauro Maggioni, and Joshua T. Vogelstein. Random Projection Forests. *arXiv e-prints*, art. arXiv:1506.03410, Jun 2015.
- [8] V. Lepetit, P. Lagger, and P. Fua. Randomized trees for real-time keypoint recognition. In *2005 IEEE Computer Society Conference on Computer Vision and Pattern Recognition (CVPR'05)*, volume 2, pages 775–781 vol. 2, June 2005. doi: 10.1109/CVPR.2005.288.
- [9] J. Gall, A. Yao, N. Razavi, L. Van Gool, and V. Lempitsky. Hough forests for object detection, tracking, and action recognition. *IEEE Transactions on Pattern Analysis and Machine Intelligence*, 33(11):2188–2202, Nov 2011. ISSN 0162-8828. doi: 10.1109/TPAMI.2011.70.
- [10] A. Bosch, A. Zisserman, and X. Munoz. Image classification using random forests and ferns. In *2007 IEEE 11th International Conference on Computer Vision*, pages 1–8, Oct 2007. doi:

- 10.1109/ICCV.2007.4409066.
- [11] J. Shotton, A. Fitzgibbon, M. Cook, T. Sharp, M. Finocchio, R. Moore, A. Kipman, and A. Blake. Real-time human pose recognition in parts from single depth images. In *CVPR 2011*, pages 1297–1304, June 2011. doi: 10.1109/CVPR.2011.5995316.
  - [12] P. Kotschieder, S. R. Buláň, H. Bischof, and M. Pelillo. Structured class-labels in random forests for semantic image labelling. In *2011 International Conference on Computer Vision*, pages 2190–2197, Nov 2011. doi: 10.1109/ICCV.2011.6126496.
  - [13] Antonio Criminisi, Jamie Shotton, and Ender Konukoglu. Decision forests: A unified framework for classification, regression, density estimation, manifold learning and semi-supervised learning. *Found. Trends. Comput. Graph. Vis.*, 7(2&#8211;3):81–227, February 2012. ISSN 1572-2740. doi: 10.1561/06000000035.
  - [14] Tyler M. Tomita, Mauro Maggioni, and Joshua T. Vogelstein. Roflmao: Robust oblique forests with linear matrix operations. In *Proceedings of the 2017 SIAM International Conference on Data Mining*, pages 498–506, 2017. doi: 10.1137/1.9781611974973.56.
  - [15] Zonghan Wu, Shirui Pan, Fengwen Chen, Guodong Long, Chengqi Zhang, and Philip S. Yu. A comprehensive survey on graph neural networks. *IEEE Transactions on Neural Networks and Learning Systems*, page 1&#211;21, 2020. ISSN 2162-2388. doi: 10.1109/tnnls.2020.2978386. URL <http://dx.doi.org/10.1109/TNNLS.2020.2978386>.
  - [16] Scott Lundberg and Su-In Lee. A unified approach to interpreting model predictions. *ArXiv*, abs/1705.07874, 2017.
  - [17] Maithra Raghu, Ben Poole, Jon Kleinberg, Surya Ganguli, and Jascha Sohl-Dickstein. On the Expressive Power of Deep Neural Networks. *arXiv:1606.05336 [cs, stat]*, June 2017. URL <http://arxiv.org/abs/1606.05336>. arXiv: 1606.05336.
  - [18] Carey E. Priebe, Joshua T. Vogelstein, Florian Engert, and Christopher M. White. Modern Machine Learning: Partition & Vote. *bioRxiv*, page 2020.04.29.068460, April 2020. doi: 10.1101/2020.04.29.068460. URL <https://www.biorxiv.org/content/10.1101/2020.04.29.068460v1>. Publisher: Cold Spring Harbor Laboratory Section: New Results.
  - [19] Misha Denil, David Matheson, and Nando De Freitas. Narrowing the gap: Random forests in theory and in practice. In Eric P. Xing and Tony Jebara, editors, *Proceedings of the 31st International Conference on Machine Learning*, volume 32 of *Proceedings of Machine Learning Research*, pages 665–673, Beijing, China, 22–24 Jun 2014. PMLR. URL <http://proceedings.mlr.press/v32/denil14.html>.
  - [20] Stefan Wager and Guenther Walther. Adaptive Concentration of Regression Trees, with Application to Random Forests. *arXiv:1503.06388 [math, stat]*, April 2016. URL <http://arxiv.org/abs/1503.06388>. arXiv: 1503.06388.
  - [21] Susan Athey, Julie Tibshirani, and Stefan Wager. Generalized random forests. *Ann. Statist.*, 47(2):1148–1178, 04 2019. doi: 10.1214/18-AOS1709. URL <https://doi.org/10.1214/18-AOS1709>.
  - [22] Gilles Louppe. Understanding random forests: From theory to practice, 2014.
  - [23] F. Pedregosa, G. Varoquaux, A. Gramfort, V. Michel, B. Thirion, O. Grisel, M. Blondel, P. Prettenhofer, R. Weiss, V. Dubourg, J. Vanderplas, A. Passos, D. Cournapeau, M. Brucher, M. Perrot, and E. Duchesnay. Scikit-learn: Machine learning in Python. *Journal of Machine Learning Research*, 12:2825–2830, 2011.
  - [24] Tianqi Chen and Carlos Guestrin. Xgboost: A scalable tree boosting system. In *Proceedings of the 22nd ACM SIGKDD International Conference on Knowledge Discovery and Data Mining*, KDD &#211;16, page 785&#211;794, New York, NY, USA, 2016. Association for Computing Machinery. ISBN 9781450342322. doi: 10.1145/2939672.2939785. URL <https://doi.org/10.1145/2939672.2939785>.
  - [25] Adam Paszke, Sam Gross, Soumith Chintala, Gregory Chanan, Edward Yang, Zachary DeVito, Zeming Lin, Alban Desmaison, Luca Antiga, and Adam Lerer. Automatic differentiation in pytorch. In *NIPS-W*, 2017.
  - [26] Laurent Younes. Diffeomorphic learning, 2018.

- [27] Roi Livni, Shai Shalev-Shwartz, and Ohad Shamir. On the computational efficiency of training neural networks. In *Proceedings of the 27th International Conference on Neural Information Processing Systems - Volume 1*, NIPS'14, pages 855–863, Cambridge, MA, USA, 2014. MIT Press.
- [28] Yann Lecun, Corinna Cortes, and Christopher J.C. Burges. *The MNIST Database of Handwritten Digits*, 1999.
- [29] Stefan Wager and Susan Athey. Estimation and Inference of Heterogeneous Treatment Effects using Random Forests. *Journal of the American Statistical Association*, 113(523):1228–1242, July 2018. ISSN 0162-1459, 1537-274X. doi: 10.1080/01621459.2017.1319839. URL <https://www.tandfonline.com/doi/full/10.1080/01621459.2017.1319839>.
- [30] Yi Lin and Yongho Jeon. Random Forests and Adaptive Nearest Neighbors. *Journal of the American Statistical Association*, 101(474):578–590, 2006. ISSN 0162-1459. URL <https://www.jstor.org/stable/27590719>. Publisher: [American Statistical Association, Taylor & Francis, Ltd.].
- [31] Richard Guo, Ronak Mehta, Jesus Arroyo, Hayden Helm, Cencheng Shen, and Joshua T. Vogelstein. Estimating Information-Theoretic Quantities with Uncertainty Forests. *arXiv:1907.00325 [cs, stat]*, November 2019. URL <http://arxiv.org/abs/1907.00325>. arXiv: 1907.00325.
- [32] Ryan Rifkin and Aldebaro Klautau. In defense of one-vs-all classification. *J. Mach. Learn. Res.*, 5: 101–141, December 2004. ISSN 1532-4435.

## Appendices.

### Appendix A. Proofs.

#### A.1 Convex Polytope Partition Results

**Theorem 1.** *A random projection tree partitions the feature space into a finite number of (possibly unbounded) convex polytopes.*

*Proof.* A convex polytope in  $d$  dimensions can be defined as the union of a finite number of half-spaces, where a halfspace is a  $d - 1$  dimensional surface defined by the linear inequality

$$a^T x \leq b$$

for fixed  $a \in \mathbb{R}^d$  and  $b \in \mathbb{R}$ . In a random projection tree, each split node  $i$  partitions the set of points at that node according to such an inequality  $a_i^T x \leq b_i$ . Consider the path of  $k$  split nodes, including the root, to a leaf  $l$  and the set of corresponding halfspace defining  $\{(a_i, b_i)\}_{i=1}^k$  terms for each split node. We see that in the feature space  $S$ , the subset that "falls into" leaf  $l$  is the solution set to

$$A_l x \leq b_l$$

where  $A_l = [a_1, \dots, a_k]^T$  and  $b_l = [b_1, \dots, b_k]^T$ .

Thus each leaf node forms a convex polytope. Additionally, note that any  $x \in S$  will deterministically end up in a leaf node (by classification of  $x$ ) as the tree is of finite depth and that all leaf node convex polytopes are mutually exclusive as the lowest common ancestor of any two leaves forms mutually exclusive sets. If the feature space is unbounded, then at least one partition must be unbounded too. Thus, a tree partitions the feature space into a finite number of possibly infinite convex polytopes. ■

**A.2 Consistency Results** The least we can ask of our classification rule  $\{g_n\}_{n=1}^\infty$  is for it to be consistent,

$$L_n \xrightarrow{P} L^* \quad \text{as } n \rightarrow \infty$$

where  $L_n$  and  $L^*$  are the expected 0-1 losses of  $g_n$  and the Bayes decision  $g^*$ , respectively.

**Oblique-splits** The Generalized Random Forest (GRF) results of Athey et al. [21] establish conditions on which random forests making axis-aligned splits lead to consistent classification rules. Critically the use of splits which may be linear combinations of features does not violate the GRF properties given our Assumptions 1-4. Specifically, the GRF [21] result relies on the consistency result of Theorem 1 in Wager and Athey [29]. We need only to verify foundations of Theorem 1 [29] that take into account the use of axis-aligned splits, those being Theorems 3 and 5 of Wager and Athey [29]. Thus, it suffices to confirm that those results are unchanged under oblique splits and our assumptions.

Theorem 3 [29] proves an asymptotic upper bound on the diameter of a leaf,  $\text{diam}(L(x))$ , by applying an asymptotic upper bound result from Lemma 2 [29] on the diameter of dimension  $j$  in the leaf,  $\text{diam}_j(L(x))$ . The leaf  $L(x)$  is a polytope formed from a combination of axis-aligned and oblique splits. Considering only the axis-aligned conditions forming  $L(x)$ , by the positive probability of splitting on each dimension per Assumption 1, the upper bound of Lemma 2 Wager and Athey [29] holds. As the addition of oblique conditions cannot increase the size of the leaf, the same upper bound holds. Similarly, the diameter  $\text{diam}(L(x))$  of the leaf is smaller than the diameter of the polytope formed from just axis-aligned conditions. By the diameter bound from Lemma 2 [20] of each feature, the upper bound of Theorem 3 [29] holds for the axis-aligned polytope and so also  $L(x)$ .

Theorem 5 [29] hinges on Lemma 4 [29] which brings up the concept of a *potential nearest neighbor* (PNN) [29] [20].

**Definition 1.**  $x_i \in \{x_1, \dots, x_s\} \in \{\mathbb{R}^p\}^s$  is a *potential nearest neighbor (PNN)* of  $x \in \mathbb{R}^p$ , if there is an axis-aligned hyperrectangle containing only  $x$  and  $x_i$ . A  $k$ -PNN set is a collection of  $k$  points and  $x$

in an axis-aligned hyperrectangle containing no other points. A predictor  $T$  for  $x$  is a  $k$ -PNN predictor if given

$$\{z\} = \{(x_1, y_1), \dots, (x_s, y_s)\} \in \{\mathbb{R}^p \times \mathcal{Y}\}^s,$$

$T$  outputs the average of the  $y_i$  among a  $k$ -PNN set of  $x$  with respect to the  $x_i$ .

In the case of oblique split decision trees, we have the following result.

**Lemma 2.** *Let  $T$  be a decision tree which makes oblique splits (including axis-aligned splits) at each interior node with finite dictionary  $\mathcal{A}$  of  $m$  vectors encoding the set of allowable oblique axes. If  $T$  has leaves between size  $k$  and  $2k - 1$ , then  $T$  is a  $k$ -PNN predictor on  $\mathbb{R}^m$ .*

*Proof.* Let  $\mathcal{X}$  denote the vector space of possible samples, where  $x \in \mathcal{X} \subset \mathbb{R}^p$ . Then  $\mathcal{A} \in \{\mathbb{R}^p\}^m$ . Let  $A \in \mathbb{R}^{p \times m}$  denote the matrix whose columns are the elements of  $\mathcal{A}$ . Then  $\mathcal{B} = A^T \mathcal{X} \subset \mathbb{R}^m$  is a vector space of dimension at most  $\min(p, m)$  in a space of dimension  $m$ . Axes in  $\mathcal{B}$  correspond to axes or oblique combinations of them in  $\mathcal{X}$  and so every oblique split in  $\mathcal{X}$  is an axis-aligned split in  $\mathcal{B}$ . The points which fall into a leaf of  $T$  are the only points which satisfy the linear system formed by the set of splits, which are the only points that fall into the hyperrectangle in  $\mathcal{B}$  defined by that system. As any decision tree making axis-aligned splits with leaves of sizes between  $k$  and  $2k - 1$  is a  $k$ -PNN predictor [30],  $T$  is thus a  $k$ -PNN predictor in  $\mathcal{B} \subset \mathbb{R}^m$ . ■

In this expanded feature space from which we can view oblique splits as axis-aligned, as in the above proof, we can scale down the marginals to be within  $[0, 1]$ . While this space no longer satisfies the Lipschitz criteria and if  $m > p$  may have a density of 0 at all points outside of the  $p$  dimensional subspace, Lemma 4 [29] requires neither of these conditions from the original assumptions. So it holds, albeit with the finite constant  $m$  instead of  $p$ . Thus Theorem 5 [29] holds with simply a modified constant which doesn't change the final established asymptotics in Theorem 1 [29]. Theorem 1 [29] so holds in our oblique forest setting and we can proceed to verify the conditions of Athey et al. [21].

**Posterior Consistency** Following from the results of Athey et al. [21] and in the spirit of Guo et al. [31], we show that random projection forests such as SPORF and MF can produce a consistent empirical estimate  $p_n(y | x)$  of the posterior  $P(Y = y | X = x)$  which we denote as  $p(y | x)$ .

**Lemma 3.** *Under Assumptions 1-4 of Section 4.2, for all  $y \in \{1, \dots, K\}$  and  $x \in \mathcal{X}$ , the honest SPORF estimate  $p_n(y | x) \xrightarrow{P} p(y | x)$  as  $n \rightarrow \infty$*

*Proof.* To estimate the posterior probability in a multiclass setting, we adopt the one-vs-all approach [32]. Let  $y$  be the fixed arbitrary class label of interest. Given our data, we seek to estimate the posterior probability  $p(y | x)$ , equivalent to estimating the conditional mean  $\mu(x) := \mathbb{E}[\mathbb{I}[Y = y] | X = x]$  for a fixed  $y$ . To follow the notation of Athey et al. [21], we frame  $\mu(x)$  as the solution to the estimation equation

$$M_\mu(x) := \mathbb{E}[\psi_{\mu(x)}(Y) | X = x] = 0$$

where the score function  $\psi_{\mu(x)}(Y)$  is defined as

$$\psi_{\mu(x)}(Y) := \mathbb{I}[Y = y] - \mu(x).$$

The solution can be estimated as the solution,  $\hat{\mu}(x)$ , to the empirical estimation equation

$$\sum_{i=1}^n \alpha_i(x) \psi_{\hat{\mu}(x)}(Y_i) = 0.$$

It follows that

$$\hat{\mu}(x) = \sum_{i=1}^n \alpha_i(x) \mathbb{I}[Y_i = y]$$



per the expansion

$$\sum_{i=1}^n \alpha_i(x) \psi_{\hat{\mu}(x)}(Y_i) = \sum_{i=1}^n \alpha_i(x) (\mathbb{I}[Y_i = y] - \hat{\mu}(x)) = \sum_{i=1}^n \alpha_i(x) \mathbb{I}[Y_i = y] - \hat{\mu}(x) = 0.$$

These weights we derive from a learned random forest. Let a forest be composed of  $B$  trees. In a single tree  $b$ , let  $l_b(x)$  denote the set of training examples at the leaf node for which  $X$  is placed. Define the weights  $\alpha_{ib}(x)$  for that tree as

$$\alpha_{ib}(x) := \frac{1}{|l_b(x)|} \mathbb{I}[x_i \in l_b(x)],$$

the normalized indicator of whether or not  $x$  and  $x_i$  exist in the same leaf. Thus the forest weights  $\alpha_i(x) = \frac{1}{B} \sum_{b=1}^B \alpha_{ib}(x)$  are simply the normalized weights across all trees.

By Theorem 3 of Generalized Random Forests (GRFs) [21], a random forest built according to the following Specification 1A and solving an estimation problem satisfying the following assumptions 1A-6A yields a consistent estimator  $p_n(y | x)$  for  $p(y | x)$ . We list these requirements and verify that they hold for honest random projection forests.

**Specification 1A:** Each tree in the forest is built with the following requirements:

- i. Is symmetric (their outputs are invariant to the permuting of the indices of the training data).
- ii. Has balanced splits (each child node receives a nonzero fraction of the observations at the parent node).
- iii. Is randomized (each feature has a nonzero probability of being split on).
- iv. The forest is honest (the posterior probabilities for a test point at a tree come from training examples not used in construction of that tree).
- v.  $s \rightarrow \infty$  and  $s/n \rightarrow 0$  where  $s$  is the number of subsampled training examples used to construct each tree and  $n$  is the total number of examples.

Specification 1A is clearly met. Subsampling of the training examples is invariant on the example indices (i) and we can asymptotically take subsamples of size  $n^\alpha$  for  $0 < \alpha < 1$  to satisfy (v). An unbalanced split is no better than any other split per the Gini split criterion and so each child node will contain a nonzero fraction of the samples at the parent (ii). Lastly, Assumptions 1 and 3 from Section 4.2 give us (iii) and (iv) respectively.

**Assumption 1A:** For fixed values  $\mu(x)$ , we assume that  $M_\mu(x)$  is Lipschitz continuous in  $x$ .

This holds per Assumption 2 from Section 4.2.

**Assumption 2A:** When  $x$  is fixed, we assume that  $M_\mu(x)$  is twice continuously differentiable in  $\mu$  with a uniformly bounded second derivative, and that  $\frac{\partial}{\partial(\mu)} M_\mu(x) |_{\mu(x)} \neq 0$  for all  $x \in \mathcal{X}$ .

This is true, as evident in the derivatives

$$\frac{\partial}{\partial \mu} M_\mu(x) = -1 \quad \text{and} \quad \frac{\partial^2}{\partial^2 \mu} M_\mu(x) = 0.$$

**Assumption 3A:** The worst-case variogram of  $\psi_\mu(Y)$  is Lipschitz-continuous in  $\mu(x)$ .

This is evident in the worse-case variogram for two solutions  $\mu$  and  $\mu'$

$$\begin{aligned} \gamma(\mu(x), \mu'(x)) &:= \sup_{x \in \mathcal{X}} \{ \text{Var}(\psi_{\mu(x)}(Y) - \psi_{\mu'(x)}(Y_i) | X = x) \} \\ &= \sup_{x \in \mathcal{X}} \{ \text{Var}(\mathbb{I}[Y = y] - \mu(x) - \mathbb{I}[Y = y] - \mu'(x) | X = x) \} \\ &= \sup_{x \in \mathcal{X}} \{ \text{Var}(\mu'(x) - \mu(x) | X = x) \} = 0 \end{aligned}$$

which is trivially Lipschitz-continuous.

**Assumption 4A:** The  $\psi$ -functions can be written as  $\psi_{\mu(x)}(Y) = \lambda(\mu(x); Y) + \xi_{\mu(x)}(g(Y))$ , such that  $\lambda$  is Lipschitz-continuous in  $\mu$ ,  $g : \{Y\} \rightarrow \mathbb{R}$  is a univariate summary of  $Y$ , and  $\xi_{\mu(x)} : \mathbb{R} \rightarrow \mathbb{R}$  is any family of monotone and bounded functions.

Clearly  $\psi_{\mu(x)}(Y)$  is linear in  $\mu(x)$  and so is a Lipschitz-continuous function in  $\mu(x)$ . The other term is 0 in this case.

**Assumption 5A:** For any weights  $\alpha_i(x)$  such that  $\sum_i \alpha_i(x) = 1$ , the estimation equation returned a minimizer  $\mu(\hat{x})$  that at least approximately solves the estimating equation

$$\left\| \sum_{i=1}^n \alpha_i(x) \psi_{\mu(\hat{x})}(Y_i) \right\|_2 \leq C \max\{\alpha_i(x)\}$$

for some constant  $C \geq 0$ .

As shown previously shown, the estimation equation is solved to equal 0.

**Assumption 6A:** The score function  $\psi_{\mu(x)}(Y)$  is a negative sub gradient of a convex function, and the expected score  $M_{\mu}(x)$  is the negative gradient of a strongly convex function.

This holds true by construction of the following convex function

$$\Psi_{\mu(x)}(Y) := \frac{1}{2}(\mathbb{I}[Y = y | X = x] - \mu(x))^2 \quad \text{such that} \quad \psi_{\mu}(Y) = -\frac{d}{d\mu} \Psi_{\mu(x)}(Y)$$

and the following strongly convex function

$$\mathbb{M}_{\mu}(x) := \frac{1}{2}(P(Y = y | x) - \mu(x))^2 \quad \text{such that} \quad M_{\mu}(x) = -\frac{d}{d\mu} \mathbb{M}_{\mu}(x)$$

**Classifier Consistency** The prior proof established consistency for each posterior probability estimate  $p_n(y | x)$ . We now proceed to show consistency for the classification rule  $g_n(x) = \operatorname{argmax}_y p_n(y | x)$ .

**Lemma 4.** *Let  $x \in \mathcal{X}$  with unique maximum  $y^* := \operatorname{argmax}_y p(y | x)$ , and define the finite sample estimate  $\hat{y} := \operatorname{argmax}_y p_n(y | x)$ . Given that  $p_n(y | x)$  is a consistent estimator for  $p(y | x)$ , then*

$$P[\hat{y} \neq y^* | x] \rightarrow 0 \quad \text{as} \quad n \rightarrow \infty$$

**Proof.** We omit the conditional for notational brevity by substituting  $p(y) := p(y | x)$  and  $p_n(y) := p_n(y | x)$ ,

$$\begin{aligned} P[\hat{y} \neq y^* | x] &= P[\max_y p_n(y) > p_n(y^*)] \\ &= P\left[\bigcup_{y \neq y^*} p_n(y) > p_n(y^*)\right] \\ &\leq \sum_{y \neq y^*} P[p_n(y) > p_n(y^*)] \\ &= \sum_{y \neq y^*} P[p_n(y) - p_n(y^*) > 0] \\ &= \sum_{y \neq y^*} P[(p_n(y) - p_n(y^*)) - (p(y) - p(y^*)) > p(y^*) - p(y)] \end{aligned}$$

Let  $\varepsilon_y := p(y^*) - p(y)$  and note that  $\varepsilon_y > 0$  for all  $y \in \mathcal{Y} \setminus \{y^*\}$  since  $y^*$  is a unique maximum. Observe that

$$\begin{aligned} &\sum_{y \neq y^*} P[(p_n(y) - p_n(y^*)) - (p(y) - p(y^*)) > \varepsilon_y] \\ &\leq \sum_{y \neq y^*} P[|(p_n(y) - p_n(y^*)) - (p(y) - p(y^*))| > \varepsilon_y] \end{aligned}$$

By the consistency of the individual posteriors, the difference of two is consistent and so since  $\mathcal{Y}$  is a finite set,

$$P[\hat{y} \neq y^* | x] \leq \sum_{y \neq y^*} P[|(p_n(y) - p_n(y^*)) - (p(y) - p(y^*))| > \varepsilon_y] \rightarrow 0 \quad \text{as } n \rightarrow \infty \quad \blacksquare$$

**Theorem 2.** *Under Assumptions 1-4, the classification rule from an honest random forest making oblique splits from the dictionary  $\mathcal{A}$  and built to the specifications of SPORF is consistent, i.e.*

$$L_n \xrightarrow{P} L^* \quad \text{as } n \rightarrow \infty$$

*Proof.* Denote the finite samples classification rule  $\hat{y} := \operatorname{argmax}_y p_n(y | x)$  as before and let  $y^* := \operatorname{argmax}_y p(y | x)$  be a unique maximum. If  $y^*$  were not unique, we would instead consider the aggregate of all such maximum classes as a pseudo class, apply the following analyses, and be confident in both  $L_n$  and  $L^*$  up to a factor equal to the reciprocal of the number aggregated classes.

To begin, for any  $\varepsilon > 0$ ,

$$\begin{aligned} P[|L_n - L^*| > \varepsilon] &= P[|p_n(\hat{y} | x) - p(y^* | x)| > \varepsilon] \\ &= P[|p_n(\hat{y} | x) - p(y^* | x)| > \varepsilon | \hat{y} = y^*] \times P[\hat{y} = y^*] + \\ &\quad P[|p_n(\hat{y} | x) - p(y^* | x)| > \varepsilon | \hat{y} \neq y^*] \times P[\hat{y} \neq y^*]. \end{aligned}$$

In the case that  $\hat{y} = y^*$ , by Lemma 3 we have convergence of the posteriors and so

$$P[|p_n(\hat{y} | x) - p(y^* | x)| > \varepsilon | \hat{y} = y^*] \rightarrow 0 \quad \text{as } n \rightarrow \infty.$$

In the case that  $\hat{y} \neq y^*$ , by Lemma 4 we have that

$$P[\hat{y} \neq y^*] \rightarrow 0 \quad \text{as } n \rightarrow \infty.$$

Since the probabilities are bounded above by one, it follows that both

$$P[|p_n(\hat{y} | X) - p(y^* | x)| > \varepsilon | \hat{y} = y^*] \times P[\hat{y} = y^*] \rightarrow 0 \quad \text{as } n \rightarrow \infty$$

and

$$P[|p_n(\hat{y} | x) - p(y^* | x)| > \varepsilon | \hat{y} \neq y^*] \times P[\hat{y} \neq y^*] \rightarrow 0 \quad \text{as } n \rightarrow \infty.$$

Thus,

$$P[|L_n - L^*| > \varepsilon] = P[|p_n(\hat{y} | x) - p(y^* | x)| > \varepsilon] \rightarrow 0 \quad \text{as } n \rightarrow \infty. \quad \blacksquare$$

Corollary 1 follows trivially from Theorem 2 with a restricted distribution of projections.

## Appendix B. Pseudocode.

---

**Algorithm 1** Learning a Manifold Oblique decision tree.

---

**Input:** (1)  $\mathcal{D}_n$ : training data (2)  $d$ : dimensionality of the projected space, (3)  $f_{\mathbf{A}}$ : distribution of the atoms, (4)  $\Theta$ : set of split eligibility criteria

**Output:** A MF decision tree  $T$

```

1: function  $T = \text{GROWTREE}(\mathbf{X}, \mathbf{y}, f_{\mathbf{A}}, \Theta)$ 
2:    $c = 1$  ▷  $c$  is the current node index
3:    $M = 1$  ▷  $M$  is the number of nodes currently existing
4:    $S^{(c)} = \text{bootstrap}(\{1, \dots, n\})$  ▷  $S^{(c)}$  is the indices of the observations at node  $c$ 
5:   while  $c < M + 1$  do ▷ visit each of the existing nodes
6:      $(\mathbf{X}', \mathbf{y}') = (\mathbf{x}_i, y_i)_{i \in S^{(c)}}$  ▷ data at the current node
7:     for  $k = 1, \dots, K$  do  $n_k^{(c)} = \sum_{i \in S^{(c)}} I[y_i = k]$  end for ▷ class counts (for classification)
8:     if  $\Theta$  satisfied then ▷ do we split this node?
9:        $\mathbf{A} = [\mathbf{a}_1 \cdots \mathbf{a}_d] \sim f_{\mathbf{A}}$  ▷ sample random  $p \times d$  matrix of atoms
10:       $\tilde{\mathbf{X}} = \mathbf{A}^T \mathbf{X}' = (\tilde{\mathbf{x}}_i)_{i \in S^{(c)}}$  ▷ random projection into new feature space
11:       $(j^*, t^*) = \text{findbestsplit}(\tilde{\mathbf{X}}, \mathbf{y}')$  ▷ Algorithm 2
12:       $S^{(M+1)} = \{i : \mathbf{a}_{j^*} \cdot \tilde{\mathbf{x}}_i \leq t^* \quad \forall i \in S^{(c)}\}$  ▷ assign to left child node
13:       $S^{(M+2)} = \{i : \mathbf{a}_{j^*} \cdot \tilde{\mathbf{x}}_i > t^* \quad \forall i \in S^{(c)}\}$  ▷ assign to right child node
14:       $\mathbf{a}^{*(c)} = \mathbf{a}_{j^*}$  ▷ store best projection for current node
15:       $\tau^{*(c)} = t^*$  ▷ store best split threshold for current node
16:       $\kappa^{(c)} = \{M + 1, M + 2\}$  ▷ node indices of children of current node
17:       $M = M + 2$  ▷ update the number of nodes that exist
18:     else
19:        $(\mathbf{a}^{*(c)}, \tau^{*(c)}, \kappa^{*(c)}) = \text{NULL}$ 
20:     end if
21:      $c = c + 1$  ▷ move to next node
22:   end while
23:   return  $(S^{(1)}, \{\mathbf{a}^{*(c)}, \tau^{*(c)}, \kappa^{(c)}, \{n_k^{(c)}\}_{k \in \mathcal{Y}}\}_{c=1}^{m-1})$ 
24: end function

```

---

---

**Algorithm 2** Finding the best node split. This function is called by growtree (Alg 1) at every split node. For each of the  $p$  dimensions in  $\mathbf{X} \in \mathbb{R}^{p \times n}$ , a binary split is assessed at each location between adjacent observations. The dimension  $j^*$  and split value  $\tau^*$  in  $j^*$  that best split the data are selected. The notion of “best” means maximizing some choice in scoring function. In classification, the scoring function is typically the reduction in Gini impurity or entropy. The increment function called within this function updates the counts in the left and right partitions as the split is incrementally moved to the right.

---

**Input:** (1)  $(\mathbf{X}, \mathbf{y}) \in \mathbb{R}^{p \times n} \times \mathcal{Y}^n$ , where  $\mathcal{Y} = \{1, \dots, K\}$

**Output:** (1) dimension  $j^*$ , (2) split value  $\tau^*$

```

1: function  $(j^*, \tau^*) = \text{FINDBESTSPPLIT}(\mathbf{X}, \mathbf{y})$ 
2:   for  $j = 1, \dots, p$  do
3:     Let  $\mathbf{x}^{(j)} = (x_1^{(j)}, \dots, x_n^{(j)})$  be the  $j$ th row of  $\mathbf{X}$ .
4:      $\{m_i^j\}_{i \in [n]} = \text{sort}(\mathbf{x}^{(j)})$  ▷  $m_i^j$  is the index of the  $i^{\text{th}}$  smallest value in  $\mathbf{x}^{(j)}$ 
5:      $t = 0$  ▷ initialize split to the left of all observations
6:      $n' = 0$  ▷ number of observations left of the current split
7:      $n'' = n$  ▷ number of observations right of the current split
8:     if (task is classification) then
9:       for  $k = 1, \dots, K$  do
10:         $n_k = \sum_{i=1}^n I[y_i = k]$  ▷ total number of observations in class  $k$ 
11:         $n'_k = 0$  ▷ number of observations in class  $k$  left of the current split
12:         $n''_k = n_k$  ▷ number of observations in class  $k$  right of the current split
13:      end for
14:    end if
15:    for  $t = 1, \dots, n - 1$  do ▷ assess split location, moving right one at a time
16:       $(\{n'_k, n''_k\}, n', n'', y_{m_t^j}) = \text{increment}(\{n'_k, n''_k\}, n', n'', y_{m_t^j})$ 
17:       $Q^{(j,t)} = \text{score}(\{n'_k, n''_k\}, n', n'')$  ▷ measure of split quality
18:    end for
19:  end for
20:   $(j^*, t^*) = \underset{j,t}{\text{argmax}} Q^{(j,t)}$ 
21:  for  $i = 0, 1$  do  $c_i = m_{t^*+i}^{j^*}$  end for
22:   $\tau^* = \frac{1}{2}(x_{c_0}^{(j^*)} + x_{c_1}^{(j^*)})$  ▷ compute the actual split location from the index  $j^*$ 
23:  return  $(j^*, \tau^*)$ 
24: end function

```

---

## Appendix C. Hyperparameters.

Table 1: ConvNet hyperparameters for each experiment.

Experiment	Classifier	Architecture Sequence
Circle	ConvNet	Conv1d(32, window=6, stride=1) MaxPool1d(window=2, stride=2) Conv1d(64, window=10, stride=1) MaxPool1d(window=2, stride=2) Dropout(p=0.5) Linear(500) Linear(2)
H/V Bars	ConvNet	Conv2d(32, window=5, stride=1) MaxPool1d(window=2, stride=2) Conv2d(64, window=5, stride=1) MaxPool1d(window=2, stride=2) Dropout(p=0.5) Linear(200) Linear(2)
Impulse	ConvNet	Conv1d(32, window=10, stride=1) MaxPool2d(window=2, stride=2) Conv2d(64, window=5, stride=1) MaxPool2d(window=2, stride=2) Dropout(p=0.5) Linear(200) Linear(2)
MNIST	ConvNet	Conv2d(32, window=5, stride=1) MaxPool2d(window=2, stride=2) Conv2d(64, window=5, stride=1) MaxPool2d(window=2, stride=2) Dropout(p=0.5) Linear(200) Linear(10)



Table 2: *scikit-learn*, *SPORF*, and *Mf* hyperparameters for each experiment.

Experiment	Classifier	Hyperparameters
Circle	Lin. SVM	$C=1$ , $\text{penalty}="l2"$ ; $\text{kernel}="linear"$ ; $\text{loss}="squared\_hinge"$
Circle	Log. Reg	$C=1$ , $\text{penalty}="l2"$
Circle	MORF	$n\_trees=500$ , $\text{max\_features}=0.5$ ; $\text{patch\_height\_max}=1$ ; $\text{patch\_height\_min}=1$ ; $\text{patch\_width\_max}=12$ ; $\text{patch\_width\_min}=3$
Circle	MLP	$\text{activation}="relu"$ ; $\alpha=0.0001$ ; $\text{hidden\_layer\_sizes}=(100,)$ ; $\text{solver}="adam"$
Circle	RF	$n\_trees=500$ , $\text{max\_features}=\text{sqrt}(n)$
Circle	XGB	$n\_boosting\_rounds = 10$ ; $\text{learning\_rate}=0.3$ ; $\text{max\_depth}=6$ ; $\text{subsample}=1$ ; $\text{tree\_method}='auto'$ (all default)
Circle	SPORF	$n\_trees=500$ , $\text{max\_features}=\text{sqrt}(n)$
Circle	SVM	$C=1$ ; $\text{gamma}=1/(n\_features*\text{Var}(X))$ ; $\text{kernel}="rbf"$
Circle	kNN	$n\_neighbors=5$ ; $p=2$
H/V Bars	Lin. SVM	$C=1$ , $\text{penalty}="l2"$ ; $\text{kernel}="linear"$ ; $\text{loss}="squared\_hinge"$
H/V Bars	Log. Reg	$C=1$ , $\text{penalty}="l2"$
H/V Bars	MORF	$n\_trees=500$ , $\text{max\_features}=\text{auto}$ ; $\text{patch\_height\_max}=2$ ; $\text{patch\_height\_min}=2$ ; $\text{patch\_width\_max}=9$ ; $\text{patch\_width\_min}=2$
H/V Bars	MLP	$\text{activation}="relu"$ ; $\alpha=0.0001$ ; $\text{hidden\_layer\_sizes}=(100,)$ ; $\text{solver}="adam"$
H/V Bars	XGB	$n\_boosting\_rounds = 10$ ; $\text{learning\_rate}=0.3$ ; $\text{max\_depth}=6$ ; $\text{subsample}=1$ ; $\text{tree\_method}='auto'$ (all default)
H/V Bars	RF	$n\_trees=500$ , $\text{max\_features}=\text{sqrt}(n)$
H/V Bars	SPORF	$n\_trees=500$ , $\text{max\_features}=\text{sqrt}(n)$
H/V Bars	SVM	$C=1$ ; $\text{gamma}=1/(n\_features*\text{Var}(X))$ ; $\text{kernel}="rbf"$
H/V Bars	kNN	$n\_neighbors=5$ ; $p=2$
Impulse	Lin. SVM	$C=1$ , $\text{penalty}="l2"$ ; $\text{kernel}="linear"$ ; $\text{loss}="squared\_hinge"$
Impulse	Log. Reg	$C=1$ , $\text{penalty}="l2"$
Impulse	MORF	$n\_trees=500$ , $\text{max\_features}=0.3$ ; $\text{patch\_height\_max}=1$ ; $\text{patch\_height\_min}=1$ ; $\text{patch\_width\_max}=12$ ; $\text{patch\_width\_min}=2$
Impulse	MLP	$\text{activation}="relu"$ ; $\alpha=0.0001$ ; $\text{hidden\_layer\_sizes}=(100,)$ ; $\text{solver}="adam"$
Impulse	RF	$n\_trees=500$ , $\text{max\_features}=\text{sqrt}(n)$
Impulse	XGB	$n\_boosting\_rounds = 10$ ; $\text{learning\_rate}=0.3$ ; $\text{max\_depth}=6$ ; $\text{subsample}=1$ ; $\text{tree\_method}='auto'$ (all default)
Impulse	SPORF	$n\_trees=500$ , $\text{max\_features}=\text{sqrt}(n)$
Impulse	SVM	$C=1$ ; $\text{gamma}=1/(n\_features*\text{Var}(X))$ ; $\text{kernel}="rbf"$
Impulse	kNN	$n\_neighbors=5$ ; $p=2$
MNIST	Lin. SVM	$C=1$ , $\text{penalty}="l2"$ ; $\text{kernel}="linear"$ ; $\text{loss}="squared\_hinge"$
MNIST	Log. Reg	$C=1$ , $\text{penalty}="l2"$
MNIST	MORF	$n\_trees=500$ , $\text{max\_features}=\text{auto}$ ; $\text{patch\_height\_max}=2$ ; $\text{patch\_height\_min}=2$ ; $\text{patch\_width\_max}=5$ ; $\text{patch\_width\_min}=2$ ;
MNIST	MLP	$\text{activation}="relu"$ ; $\alpha=0.0001$ ; $\text{hidden\_layer\_sizes}=(100,)$ ; $\text{solver}="adam"$
MNIST	XGB	$n\_boosting\_rounds = 10$ ; $\text{learning\_rate}=0.3$ ; $\text{max\_depth}=6$ ; $\text{subsample}=1$ ; $\text{tree\_method}='auto'$ (all default)
MNIST	RF	$n\_trees=500$ , $\text{max\_features}=\text{sqrt}(n)$
MNIST	SPORF	$n\_trees=500$ , $\text{max\_features}=\text{sqrt}(n)$
MNIST	SVM	$C=1$ ; $\text{gamma}=1/(n\_features*\text{Var}(X))$ ; $\text{kernel}="rbf"$
MNIST	kNN	$n\_neighbors=5$ ; $p=2$